

# CALIBRATION AND EXPERIMENTS OF THE DISCRETE ELEMENT SIMULATION PARAMETERS FOR RICE BUD DAMAGE

## 水稻种芽损伤离散元仿真参数标定与试验

Xiangqian DONG\*, Huina ZHENG, Xuan JIA, Yonglei LI, Jiannong SONG, Jicheng WANG<sup>1</sup>

China Agricultural University, College of Engineering, Beijing / China

Tel:0086-010-62737502; E-mail: dxq0558@126.com

Corresponding authors: Xiangqian Dong

DOI: <https://doi.org/10.35633/inmateh-68-65>

**Keywords:** Rice bud; Seed bud cutting; Discrete element method; Parameter calibration

**ABSTRACT** Rice buds are easily bruised or broken during sowing, which affects the seedling rate, and the discrete element simulation of rice buds lacks an accurate model in this process. The EDEM simulation software was used to calibrate the parameters of the discrete element simulation model for different states of rice bud seeds damage. The Hertz-Mindlin model was used to simulate the accumulation of rice bud seeds. Through a series of tests, the interspecific static friction factor was 0.644, and the rolling friction factor was 0.062. The normal contact stiffness and tangential contact stiffness were determined for the bud germination state and the 1-3 mm bud length state, respectively, by using the meta-particle function to build rice seed sprouts and applying the bonding model to conduct Box - Behnken response surface tests for shear damage of rice seed sprouts. Finally, experiments were carried out with a hole-belt-type seed meter. The results showed that under different belt speeds, the relative error between the measured value and the simulated value of the rice bud damage rate was not more than 0.9%, indicating that the calibration parameters were accurate and reliable.

### 摘要

水稻在播种过程中种芽易被碰伤或折断影响成苗率,且此水稻种芽离散元仿真缺乏准确模型。以不同状态水稻种芽为研究对象,利用 EDEM 仿真软件开展水稻种芽损伤离散元仿真模型参数标定研究。应用 Hertz - Mindlin 模型进行水稻种芽堆积仿真试验,通过一系列试验,确定了水稻种芽颗粒间静摩擦因数为 0.644,种间滚动摩擦因数为 0.062。利用 meta-particle 功能建立水稻种芽并应用 Hertz - Mindlin with bonding 粘结模型开展水稻种芽剪切破坏离散元单因素和 Box - Behnken 响应曲面试验,确定了破胸状态与芽长 1-3mm 状态时法向接触刚度分别为  $1.07 \times 10^{+08} \text{N/m}$ 、 $8.99 \times 10^{+07} \text{N/m}$ ,切向接触刚度分别为  $9.05 \times 10^{+07} \text{Pa}$ 、 $8.24 \times 10^{+07} \text{Pa}$ 。采用型孔带式排种器进行了试验验证,结果表明,在不同带速条件下,水稻种芽损伤率实测值与仿真值的相对误差不大于 0.9%,说明标定参数准确可靠。

### INTRODUCTION

When sowing rice seedlings, it is necessary to germinate the seeds. Research shows that it is suitable to sow rice seeds in a bud germination state or when the bud length reaches 1~3 mm. Germinated rice seeds differ from dry-based moisture-content rice seeds in terms of morphology, water content and mobility, and rice bud seeds are a more structurally complex agricultural material. Structurally, rice bud seeds consist of two parts: the rice matrix, which includes the brown rice and the rice husk, and the buds, which are developed from the endosperm by consuming nutrients in the embryo. Differences in physical properties due to differences in composition. Rice bud seeds are subject to pressure and impact from outside and between seeds during the sowing process. If the force is too great, the buds will be damaged, and the rice seedling emergence rate will be affected. Therefore, it is necessary to analyse the rice matrix and bud attachment force.

In recent years, EDEM, a simulation software based on the discrete element method (DEM), has been widely used to study agricultural equipment. The accuracy of the model building and the various material parameters in DEM simulations is crucial to the simulation process.

---

Xiangqian Dong, SE.Ph.D. Eng; Huina Zheng, M.S. Stud. Eng; Xuan Jia, Ph.D.Stud. Eng; Yonglei Li, Assoc. Prof.Ph.D. Eng; Jiannong Song, Prof.ph.D. Eng; Jicheng Wang, ST.

Therefore, DEM models and contact parameters for materials such as buckwheat seeds (Xu *et al.*, 2021), mixed biomass sawdust (Xun *et al.*, 2022), wheat straw-soil mixtures (Gao *et al.*, 2022), king grass (Huan *et al.*, 2022) and sunflower seed particles (Wang *et al.*, 2022) had been extensively investigated by many scholars.

Some scholars have also used discrete element numerical simulation methods to research on rice seed-metering devices, mainly for modelling and simulation analysis of dry rice seeds. Rice dry seeds (Zhang *et al.*, 2020) were filled by a bonded polymerisation model formed by spherical particles with different filling radii. The optimum filling particle radius was sought by stacking angle tests. Lu *et al.* (Lu *et al.*, 2018) constructed a DEM for rice bud seeds and calibrated the main contact parameters of the discrete element for rice bud seeds at different water contents. In this model, the buds are integrated with the matrix. The above studies mainly focused on the dry rice seeds or the matrix and bud as one rice bud seed to build simulation models; none of them analysed the connection force between the matrix and bud.

The Hertz-Mindlin with bonding model can simulate the breakage and fracture of crops during harvesting and processing and is widely used in the field of agricultural material modelling (Shaikh *et al.*, 2021; Zhang *et al.*, 2022). Coetzee *et al.* (Coetzee *et al.*, 2013) measured the material properties of grapes through a series of experiments, modelled a bunch of grapes using the bonding model in the discrete element approach, and used a simplified corer model to simulate a peeler to separate the fruit from the stalk.

Yitao Liao *et al.* (Liao *et al.*, 2020) developed a basic contact model and bonding model for forage rape stalks at the Carex stage and calibrated them using stacking angle and shear force. Du *et al.* (Du *et al.*, 2021) trained Bonding models for calibrated envelope fertilizers by uniaxial compression actual and simulation tests and full-factor tests with PSO-BP neural networks. Zhang *et al.* (Zhang *et al.*, 2022) used a BPM model to calibrate a simulation model of the water chestnut peeling and dicing process.

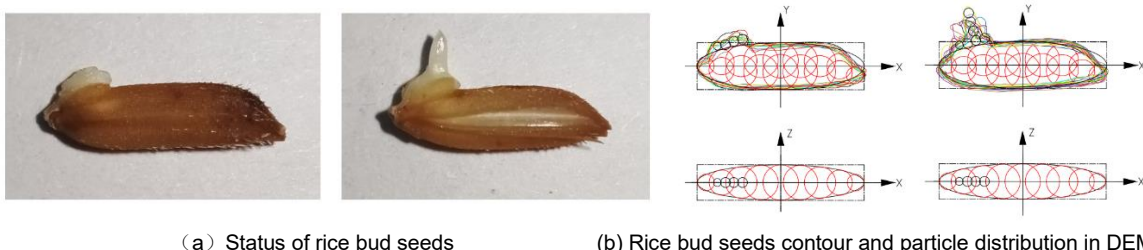
In this paper, discrete element models (DEM) were constructed for rice bud seeds in the bud germination state and the bud lengths of 1 mm, 2 mm and 3 mm. The Hertz-Mindlin model was applied to simulate rice shoot seed stacking, and the main influencing factors were selected to determine the basic contact parameters. The accuracy of the DEM and the parameters calibrated was verified in a bench test using a type-hole belt seed-metering device. The results of the study can provide a new idea for discrete element modelling of rice bud seeds and provide a theoretical basis for analysing the movement, stress state and breakage of rice bud seeds during mechanized seeding in order to provide a database for the optimal design of operational parameters of rice precision seed dispensers.

## MATERIALS AND METHODS

### The DEM model of rice bud seeds

Randomly take 100 grains of Jing Gangruanzhan from Jiangxi province and measure the length, width and thickness with vernier callipers. Then, ten seeds of each of the three-dimensional dimensions of the broken breast and sprouted state were selected and placed flat, and the image acquisition of the rice sprouted seeds was carried out as shown in Figure 1(a).

The contours were extracted and combined to determine the location of the broken breast and buds, and the Hertz - Mindlin model was used to establish four states of broken breast, bud length 1 mm, 2 mm, and 3 mm, as shown in Figure 1(b). The last three states are represented in one model, with different numbers of particles selected according to the bud length. The radius and X-directional coordinates of the ball are determined in the XZ plane, and the Y-directional coordinates are defined in the XY plane when modelling the rice matrix. The coordinate values are determined according to the number of particles and the coordinate formula. The optimal solution is selected based on the computational efficiency and the degree of model fit. Finally, there is a gap between the bud and matrix particles to prepare for the subsequent addition of bonding bonds in the shear model.



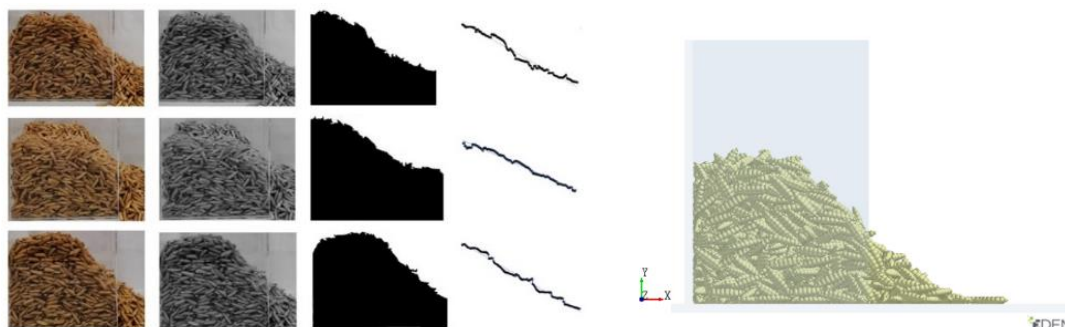
(a) Status of rice bud seeds

(b) Rice bud seeds contour and particle distribution in DEM

**Fig. 1 - Rice bud seeds**

**Stacking angle of rice bud seeds**

Rice sprout seeds with surface moisture suitable for sowing were selected for the stacking test using the sidewall collapse method. The Jing Gangruanzhan mentioned above was selected as the test material, and the right side of the rice bud seeds collapsed to form the stacking angle during the test. After all the seeds were stationary, the front view of the seed pile was taken with a high-definition camera, and the pile images were grayscale processed and binarized. The image boundary pixel points were extracted and fitted by Matlab, as shown in Figure 2(a). Three replicate tests were conducted at one-hour intervals, and the average pile-up angle for the physical test of rice shoot seeds was obtained as 41.41°.



(a) Edge contour extraction process of stacking angle (b) Angle of repose simulation model for rice bud seeds

**Fig. 2 - Stacking angle of rice bud seeds**

The model was drawn in EDEM software according to the actual single-sided extractable topless cube dimensions. Polygon virtual planes were created at the top of the cube for the dynamic generation of 1000 rice bud seeds at a rate of 1500/s. Rice bud seeds were established according to the DEM above, and the number ratios matched the actual test ratios. In order to ensure that the particles fall quickly, the initial falling speed of particles is set to 1 m/s. After the particles are generated and stabilized, the right baffle is set to be lifted upward with a speed of 1 m/s. The simulated particles collapse from the right side to finally form a stable pile of particles, the model is shown in Figure2(b), and the parameters are set as shown in Table 1.

**Table 1**

**Parameters of angle of repose simulation model for rice bud seeds**

Parameter	Poisson's ratio	Real density	Shear modulus	Collision recovery factor with rice bud seeds	Coefficient of static friction with rice bud seeds	Coefficient of rolling friction with rice bud seeds
	—	[kg/m <sup>3</sup> ]	[Pa]	—	—	—
Rice bud seeds	0.25	1060	1.08e+08	0.46	0.42-0.7 <sup>a</sup>	0.04-0.1 <sup>a</sup>
Plexiglass	0.23	1200	2.35e+08	0.5	0.24	0.22

Note: a indicates that this item is a test variable, as below.

**Shear force of rice bud (actual)**

The goal was to obtain the mechanical properties between the rice matrix and the seed bud. First, a tool probe sheared the joint between the matrix and the seed bud on an XT plus texturizer (stable micro systems, UK) close to the side of the matrix. Then, the maximum load of shear damage during loading was recorded as a reference value. Clamp the rice substrate by hand with a pair of sharp-jaw pliers held in place by a homemade jig. Adjust the platform and jig position so that the part of the substrate attached to the seed shoot is directly below the probe, as shown in Figure 3(a).

Two kinds of conventional rice, Jing Gangruanzhan and Feng Yu8, and three kinds of hybrid rice, Tai You398, Hua Zhongyou1 and Yi You2108, were selected. Prefabricated bud species of different states were selected with stainless steel A/MORS probes (thickness 0.3 mm, width 7 mm) and loaded at a speed of 5×10e-4 m/s with a drop distance of 10 mm. The test was repeated ten times for each species in different states, the average value of the maximum shear force was counted, and the coefficient of variation was less than 0.25. It can be seen from Figure 3(b) that although there were differences in the shear force between the rice matrix and bud connection part in different states of different varieties, the shear force was the largest when each variety is in the bud germination state. On the other hand, the shear force tends to be the same and less than the bud germination state when the bud length is 1-3 mm.

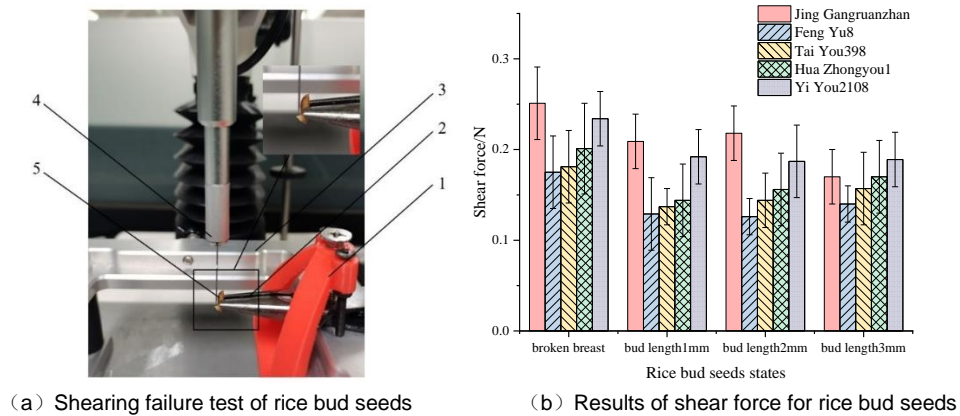


**Fig. 3 Shearing failure tests and results of rice bud seeds**

1- Fixture; 2- Sharp-jaw plier; 3- Platform; 4- Tool probe; 5- Rice bud seed

**Shear force of rice bud (simulation)**

The rice matrix and buds were modelled separately and combined into rice bud seeds using the meta-particle function, and the contour model was consistent with the above. Based on the Hertz-Mindlin model, the Hertz-Mindlin with bonding model was used to simulate the problems of material fragmentation and fracture by adding inter-particle bonding between the rice matrix and buds. The contact radius  $R_B$  is 30% of the physical radius  $R$ , and the bond radius is 1.2~2.0 times of the contact radius. The bond is broken when the shear force between the particles reaches the set limit force, and the bond no longer exists between the damaged matrix and buds, which can be used for the simulation study of the damage process of rice seed buds. The particles were used to simulate rice bud seeds, and the bond was broken when the shear force experienced between the particles reached the set limit force. The schematic diagram of particle bonding is shown in Figure 4(a).

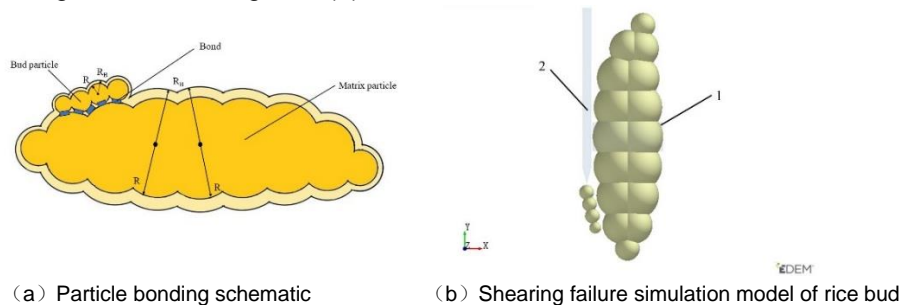


**Fig. 4 Shearing failure test of rice bud seeds**

1- Thin-walled cylinder; 2- Tool probe

A particle factory was established to generate a rice bud seed, and the coordinates of the matrix particle and bud particle were extracted. Then the tool model was created by the 3D software SOLIDWORKS and imported into EDEM. Finally, a thin-walled cylinder with a radius of 1.21 mm was created in EDEM to fix the rice bud seed at the centre of the rice matrix. The tool motion speed was the same as the actual one, and the direction was vertical downwards. A simulation model of the shear damage of the buds was created, as shown in Figure 4 (b), and a fixed time step of 3% was set for the simulation calculation. The primary contact parameters of the simulation model are shown in Table 2.

**Table 2**

Parameters of shearing failure simulation model and bonding for rice bud		
Type	Parameter	Values
Tool	Density/(kg·m <sup>-3</sup> )	7850
	Poisson ratio	0.3
	Shear modulus/GPa	7.9
Tool-Rice bud seeds	Coefficient of restitution	0.42
	Coefficient of static friction	0.52
	Coefficient of rolling friction	0.01
Bonding parameters	Normal contact stiffness	10 <sup>6</sup> ~10 <sup>8a</sup>
	Tangential contact stiffness	10 <sup>6</sup> ~10 <sup>8a</sup>
	Critical normal stress	10 <sup>6</sup> ~10 <sup>8a</sup>
	Critical tangential stress	10 <sup>6</sup> ~10 <sup>8a</sup>

**RESULTS**

**Design and analysis of stacking angle response surface tests**

The most important factors influencing the stacking angle are the interspecies static friction factor  $X_1$  and the interspecies rolling friction factor  $X_2$  by the Plackett Burman pre-test. The steepest climb test is conducted for the screened main factors to determine the optimal value proximity area. To obtain the optimal contact parameter combinations, a central composite test design was applied to Design-Expert. The stacking angle tests were performed for 11 sets of parameter combinations, of which three sets were central horizontal repetition tests. The factor coding values are shown in Table 3, and the experimental design scheme and results are shown in Table 4.

**Table 3**

**Coding of simulation test factor**

Code	-1.414	-1	0	1	1.414
$X_1$	0.42	0.46	0.56	0.66	0.7
$X_2$	0.04	0.049	0.07	0.091	0.1

**Table 4**

**Design and results of center compound test**

Test No.	$X_1$	$X_2$	Stacking angle $\theta/^\circ$	Relative error $\delta/\%$
1	-1	-1	37.43	9.61
2	1	-1	38.15	7.87
3	-1	1	39.49	4.64
4	1	1	51.14	23.5
5	-1.414	0	39.45	4.73
6	1.414	0	44.96	8.57
7	0	-1.414	37.53	9.37
8	0	1.414	46.34	11.9
9	0	0	40.4	2.44
10	0	0	40.97	1.06
11	0	0	40.58	2

**Table 5**

**Analysis of variance in regression model of response surface optimization test for stacking angle**

Source	Sum of square	df	Sum of mean square	F-value	P-value
model	178.29	5	35.66	42.82	0.0004**
$X_1$	50.81	1	50.81	61.02	0.0006**
$X_2$	94.59	1	94.59	113.59	0.0001**
$X_1X_2$	29.87	1	29.87	35.86	0.0019**
$X_1^2$	2.37	1	2.37	2.85	0.1523
$X_2^2$	1.49	1	1.49	1.79	0.2391
Residual	4.16	5	0.8328		
Lack of fit	3.99	3	1.33	15.68	0.0605
Pure error	0.1698	2	0.0849		

Note: \* indicates that this item has significant effect on the result ( $P \leq 0.05$ ),  
 \*\* indicates that this item has extremely significant effect on the result ( $P \leq 0.01$ ).

As shown in Table 5 of the ANOVA results, the regression model  $P=0.0004$ , the lack of fit  $P=0.0605$ , the coefficient of determination  $R^2 = 0.9772$ , and the coefficient of determination was close to 1, indicating that the regression equation was a good fit. From Table 5, it can be seen that  $X_1$ ,  $X_2$  and  $X_1X_2$  had highly significant effects on the stacking angle of rice bud seeds,  $X_1^2$  and  $X_2^2$  had insignificant effects on the stacking angle of rice bud seeds, and the effects were ranked from most significant to least:  $X_2$ ,  $X_1$  and  $X_1X_2$ . The stacking angle response surface is shown in Figure 5.



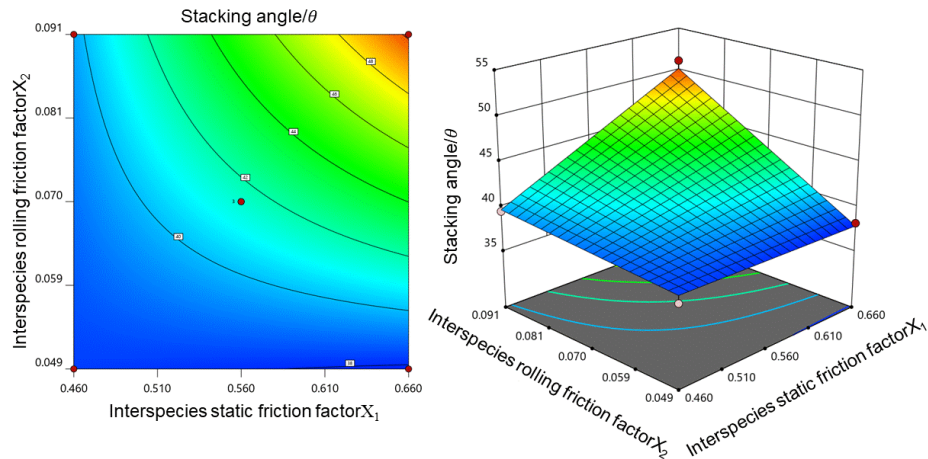


Fig. 5 - Response surface of stacking angle

The stacking angle ( $\theta$ ) regression model with the interspecies static friction factor  $X_1$  and interspecies rolling friction factor  $X_2$  was developed by fitting a binary regression to the data in Table 5 and removing the insignificant factors, as shown in equation (1).

$$\theta = 66.93 - 65.88x_1 - 564.92x_2 + 1301.09x_1x_2 \tag{1}$$

**Design and analysis of response surface tests for bonding parameters**

According to the Hertz - Mindlin principles with the bonding model, the bond breakage between the particles is the result of a combined effect. The bond radius of 0.5 mm and the order of magnitude of normal contact stiffness, tangential contact stiffness, critical normal stress, and critical tangential stress were determined based on the single-factor pre-test. Box - Behnken Design (BBD) of rice buds shear simulation tests were performed using the parameter values in Table 6 and the bonding parameter values determined in the previous section. The bonding parameters were coded as shown in Table 6. A total of 27 sets of simulations were conducted, with three replications set at the central level. The experimental design and simulation results are shown in Table 7.

Table 6

**Coding of bonding parameters**

Code	$X_3$	$X_4$	$X_5$	$X_6$
	[N/m]	[N/m]	[Pa]	[Pa]
-1	$0.30 \times 10^{+08}$	$0.37 \times 10^{+08}$	$0.05 \times 10^{+06}$	$0.05 \times 10^{+06}$
0	$1.10 \times 10^{+08}$	$1.07 \times 10^{+08}$	$1.05 \times 10^{+06}$	$1.05 \times 10^{+06}$
1	$1.90 \times 10^{+08}$	$1.77 \times 10^{+08}$	$2.05 \times 10^{+06}$	$2.05 \times 10^{+06}$

Table 7

**Response surface test design and results of bonding parameters**

Test No.	$X_3$	$X_4$	$X_5$	$X_6$	Shear force / [N]
1	-1	-1	0	0	0.0706
2	1	-1	0	0	0.31
3	-1	1	0	0	0.0441
4	1	1	0	0	0.43
5	0	0	-1	-1	0.2552
6	0	0	1	-1	0.2546
7	0	0	-1	1	0.251
8	0	0	1	1	0.256
9	-1	0	0	-1	0.034
10	1	0	0	-1	0.411
11	-1	0	0	1	0.034
12	1	0	0	1	0.416
13	0	-1	-1	0	0.239
14	0	1	-1	0	0.1726
15	0	-1	1	0	0.239
16	0	1	1	0	0.1788
17	-1	0	-1	0	0.0339

18	1	0	-1	0	0.4170
19	-1	0	1	0	0.034
20	1	0	1	0	0.414
21	0	-1	0	-1	0.238
22	0	1	0	-1	0.1746
23	0	-1	0	1	0.239
24	0	1	0	1	0.1788
25	0	0	0	0	0.2636
26	0	0	0	0	0.2518
27	0	0	0	0	0.2729

Table 8

**Analysis of variance in regression model of response surface optimization test for shearing force**

Source	Sum of square	df	Sum of mean square	F-value	P-value
model	0.4006	14	0.0286	26.35	<0.0001**
$X_3$	0.3843	1	0.3843	353.91	<0.0001**
$X_4$	0.0020	1	0.0020	1.88	0.1949
$X_5$	4.941e-06	1	4.941e-06	0.0046	0.9473
$X_6$	4.563e-05	1	4.563e-05	0.0042	0.9494
$X_3 X_4$	0.0054	1	0.0054	4.94	0.0462*
$X_3 X_5$	2.403e-06	1	2.403e-06	0.0022	0.9633
$X_3 X_6$	6.250e-06	1	6.250e-06	0.0058	0.9408
$X_4 X_5$	9.610e-06	1	9.610e-06	0.0089	0.9266
$X_4 X_6$	2.560e-06	1	2.560e-06	0.0024	0.9621
$X_5 X_6$	7.840e-06	1	7.840e-06	0.0072	0.9337
$X_3^2$	0.0026	1	0.0026	2.42	0.1458
$X_4^2$	0.0081	1	0.0081	7.45	0.0183*
$X_5^2$	0.0005	1	0.0005	0.5040	0.4913
$X_6^2$	0.0006	1	0.0006	0.5407	0.4763
Residual	0.0130	12	0.0011		
Lack of fit	0.0128	10	0.0013	11.45	0.0829
Pure Error	0.0002	2	0.0001		

The analysis of variance for the model data is shown in Table 8. The effect of  $X_3$  on shear force of rice buds was significant within the range of different numerical levels of bonding model parameters described in Table 8.  $X_3 X_4$  had a significant effect on the shear force, while the rest of the interaction terms did not have a significant effect on shear force; the secondary term  $X_4^2$  had a significant effect on the shear force, while the rest of the secondary terms did not have a significant effect. Figure 6 shows the effect of the interaction between  $X_3$  and  $X_4$  on the shear force. The  $X_3$  effect surface curve is steeper than the  $X_4$  direction, indicating a more significant effect on the  $X_3$  shear force than  $X_4$ .

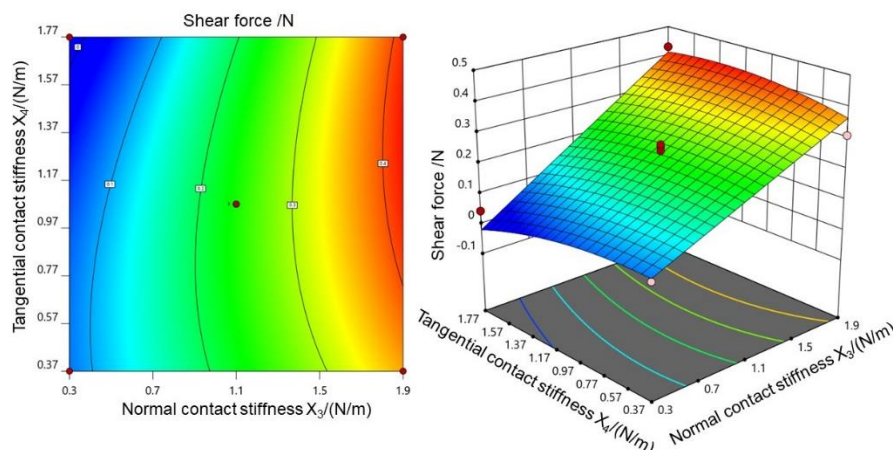


Fig. 6 - Response surface of shearing failure

For the obtained test results, Design-expert software was applied to fit the test results to a multiple regression analysis. For the regression model obtained, the final regression model for shear was obtained by excluding the non-significant term at  $P > 0.05$  from the ANOVA, as shown in equation (2).

$$f = 0.02 + 0.154x_3 + 0.042x_4 + 0.065x_3x_4 - 0.062x_4^2 \tag{2}$$

The fitted multiple regression model  $P < 0.0001$  indicated that the shear force was highly significant concerning the fitted quadratic regression equation. The coefficient of determination of the fitted model  $R^2 = 0.9619$ ,  $R^2_{adj} = 0.9549$ , and the accuracy of the model in Design-expert was 38, indicating that the quadratic polynomial regression equation was a good fit. The shear force values obtained from the actual shear test were substituted into equation (2) to obtain multiple sets of optimised solutions for simulation. In the case of approximately the same shear displacement, a set of bonding parameters with the closest shear force values in the simulation test and the actual shear test were selected: bond radius of 0.5 mm, normal contact stiffness of  $1.07 \times 10^8 \text{ N/m}$ , tangential contact stiffness of  $9.05 \times 10^7 \text{ N/m}$ , critical normal stress of  $1.87 \times 10^5 \text{ Pa}$ , critical tangential stress of  $1.82 \times 10^5 \text{ Pa}$ . A comparison of the simulated and measured shear curves is shown in Figure 7.

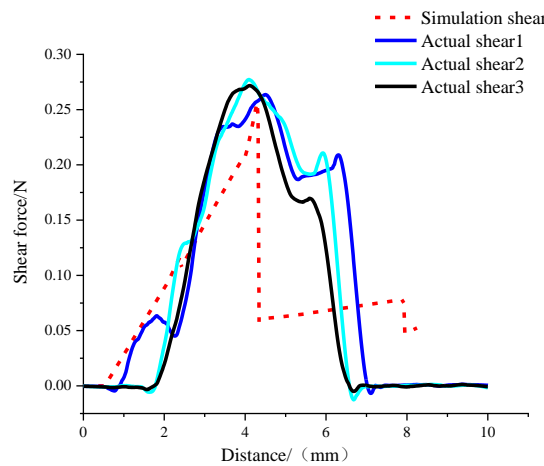


Fig. 7 - Force-displacement curve of shearing failure for simulation-test

The same method was used to calibrate the optimum parameters for rice seeds with bud lengths of 1-3 mm: bond radius of 0.5 mm, normal contact stiffness of  $8.99 \times 10^7 \text{ N/m}$ , tangential contact stiffness of  $8.24 \times 10^7 \text{ N/m}$ , critical normal stress of  $1.24 \times 10^5 \text{ Pa}$  and critical tangential stress of  $6.49 \times 10^5 \text{ Pa}$ .

**Bud damage test verification**

To further verify the reliability of the DEM and simulation parameters for rice bud seeds, a type-hole belt seed-metering device was built for bench tests. The measured and simulated values of the bud damage rate were compared at belt speeds of 0.05, 0.08, 0.11, 0.14 and 0.17 m/s, respectively, using the bud damage rate as the test index. The Jing Gangruanzhan calibrated above was selected for a bench test, with the seed box made of acrylic and the belt made of PVC, as shown in Figure 8 (a).

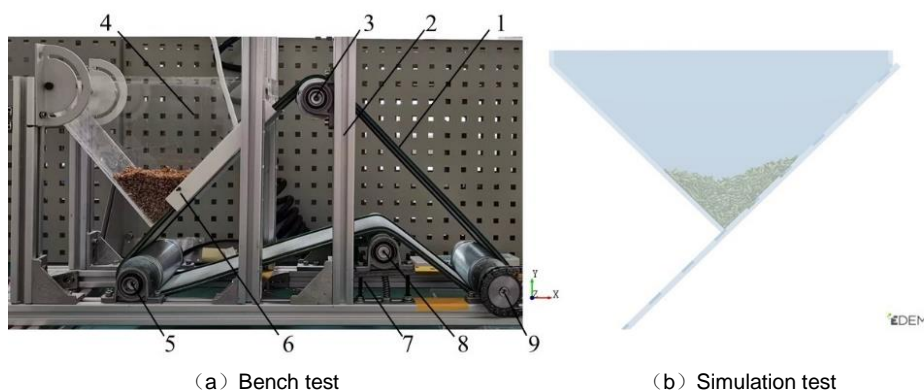


Fig. 8 - Verification test

- 1- Type hole belt; 2- Frame; 3- Slave roller I; 4- Seed box; 5- Slave roller II; 6- Guide support slot; 7- Tensioning device; 8- Tensioning roller; 9- Active rollers



For the experiment, 10000 rice bud seeds of Jing Gangruanzhan were prepared and placed in the seed box, and 500 seeds were randomly selected to count the number of different rice states to determine the overall proportion. The controller was switched on and off, the movement was stopped after 10 s, and 500 seeds were randomly selected to count the damage rate of rice buds. The seed-metering device mainly relies on the principle of circulating friction of the seed layer to drive rice bud seed filling. After the seeds entered the hole, they remained stationary with the belt in a stable state. The main force and damage to the buds occurred mainly in the seed-filling process, so the seed-filling process was simulated only. In order to reduce the amount of simulation calculation, the seed box and belt were scaled according to a specific ratio based on the actual test, and the number of simulated rice bud seeds was 1000. The calibrated and measured contact parameters were imported into the discrete element software EDEM. The simulation test was conducted under the same conditions as the bench test to count the number of broken bonds. The simulation test is shown in Figure 8 (b).

Figure 9 shows the measured and simulated values of the bud damage rate at different belt speeds. From Fig.9, the measured and simulated values of bud damage rate increased with the increase of belt speed, and the maximum error between them did not exceed 0.9%.

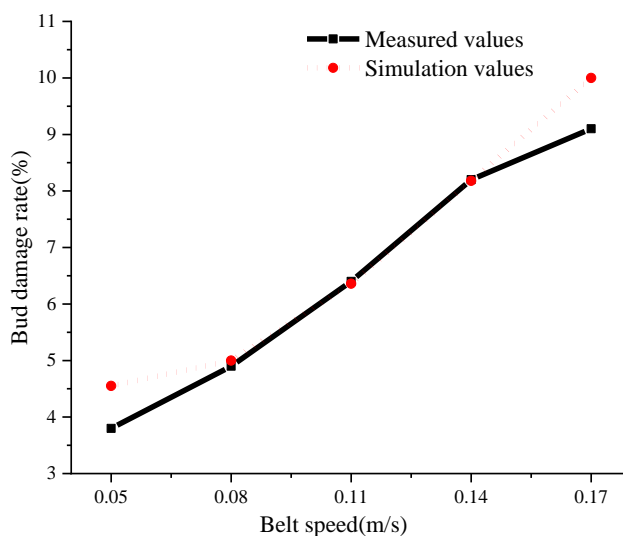


Fig. 9 - Measured and simulated values of damage rate of buds at different belt speeds

## CONCLUSIONS

The physical stacking test of rice bud seeds was carried out using the sidewall collapse method. The stacking angle images were processed using MATLAB to obtain edge profiles, which were linearly fitted to obtain a mean stacking angle of  $41.41^\circ$ . A central composite experimental design was applied to Design-Expert to produce an optimized solution. The parameters were 0.644 for the static friction factor between rice bud seeds and 0.062 for the rolling friction factor between seeds. The model was built using the calibrated parameters to simulate the stacking angle, and the relative error between the simulated and measured values was 0.17%.

A Box-Behnken response surface test was carried out to establish a regression model between shear force and two significant parameters: normal contact stiffness and tangential contact stiffness, using the broken chest state of Jing Gangruanzhan as an example. Optimal parameter combinations were in order:  $1.07 \times 10^8$  N/m,  $9.05 \times 10^7$  N/m. The parameter combinations were  $8.99 \times 10^7$  N/m and  $8.24 \times 10^7$  N/m when the same method was used to calibrate bud lengths of 1-3 mm.

A type-hole belt seed-metering device was built for bench testing and simulated in EDEM software for test analysis. The results showed that the maximum error between the measured and simulated values of the bud damage rate did not exceed 0.9% at different belt speeds. Therefore, this DEM of rice bud seeds, contact parameters and bonding parameters between the matrix and buds can be used for discrete element simulation tests.

## ACKNOWLEDGEMENT

This research was supported by Technology for the Economy 2020 (2020YFF0426562-2).

## REFERENCES

- [1] Bing Xu, Yanqing Zhang, Qingliang Cui, Shaobo Ye, Fan Zhao., (2021), Construction of a discrete element model of buckwheat seeds and calibration of parameters, *INMATEH Agricultural Engineering*, Bucharest/Romania, vol.64, no.2, ISSN, pp.175-184.
- [2] Corné J. Coetzee, Stephanus G. Lombard., (2013), The destemming of grapes: Experiments and discrete element modelling, *Biosystems Engineering*, vol.114, no.3, ISSN, pp.232-248.
- [3] Fangyuan Lu, Xu Ma, Suiyan Tan, Lintao Chen, Lingchao Zeng, Pei An., (2018), Simulative calibrate and experiment on main contact parameters of discrete elements for rice bud seeds (水稻芽种离散元主要接触参数仿真标定与试验), *Transactions of the Chinese Society for Agricultural Machinery*, Madison/Wisconsin, vol.49, no.2, ISSN, pp.93-99.
- [4] Guozhong Zhang, Liming Chen, Haopeng Liu, Zhao Dong, Qinghong Zhang, Yong Zhou., (2022), Calibration and experiments of the discrete element simulation parameters for water chestnut (荸荠离散元仿真参数标定与试验), *Transactions of the Chinese Society of Agricultural Engineering*, Madison/Wisconsin, vol.38, no.11, ISSN, pp.41-50.
- [5] Lei Zhang, Yibin Zhai, Jianneng Chen, Zhien Zhang, Shouzhi Huang., (2022), Optimization design and performance study of a subsoiler underlying the tea garden subsoiling mechanism based on bionics and EDEM, *Soil & Tillage Research*, Netherlands, vol.191, no.3, ISSN, pp.183-192.
- [6] Rongfang Zhang, Wei Jiao, Jilei Zhou, Bing Qi, Hu Liu, Qianqian Xia., (2020), Parameter calibration and experiment of rice seeds discrete element model with different filling particle radius (不同填充颗粒半径水稻种子离散元模型参数标定), *Transactions of the Chinese Society for Agricultural Machinery*, Madison/Wisconsin, vol.51, no. S1, ISSN, pp.227-235.
- [7] Sher Ali Shaikh, Yaoming Li, Zheng Ma, Farman Ali Chandio, Mazhar Hussain Tunio, Zhenwei Liang, Kashif Ali Solangi., (2021), Discrete element method (DEM) simulation of single grouser shoe-soil interaction at varied moisture contents, *Computers and Electronics in Agriculture*, Netherlands, vol.191, no.1, ISSN, pp.106538.
- [8] Shuai Wang, Zhihong Yu, Aorigeleo, Wenjie Zhang., (2022), Study on the modelling method of the sunflower seed particles based on the discrete element method, *Computers and Electronics in Agriculture*, Netherlands, vol.65, no.3, ISSN, pp.183-192.
- [9] Tao Jiang, Chongyou Wu, Qing Tang., (2018), Simulation study of wheat straw cutting based on ANSYS and EDEM (基于 ANSYS 和 EDEM 的小麦茎秆切割仿真研究), *Jiangsu Agricultural Sciences*, Madison/Wisconsin, vol.46, no.17, ISSN, pp.231-234.
- [10] Xin Du, Cailing Liu, Meng Jiang, Hao Yuan, Lei Dai, Fanglin Li, Zhanpeng Gao., (2021), Calibration of bonding model parameters for coated fertilizers based on PSO-BP neural network, *INMATEH Agricultural Engineering*, Bucharest/Romania, vol.65, no.3, ISSN, pp.255-264.
- [11] Xiaolong Huan, Decheng Wang, Yong You, Wenpeng Ma, Lu Zhu, Sibiao Li., (2022), Establishment and calibration of discrete element model of king grass stalk based on throwing test, *INMATEH Agricultural Engineering*, Bucharest/Romania, vol.66, no.1, ISSN, pp.19-30.
- [12] Xun Gong, Xuwei Bai, Haibo Huang, Fengyu Zhang, Yuanjuan Gong, Desheng Wei., (2022), DEM parameters calibration of mixed biomass sawdust model with multi-response indicators, *INMATEH Agricultural Engineering*, Bucharest/ Romania, vol.65, no.3, ISSN, pp.183-192.
- [13] Yitao Liao, Qingxi Liao, Yu Zhou, Zaiteng Wang, Yajun Jiang, Fang Liang., (2020), Parameters calibration of discrete element model of fodder rape crop harvest in bolting stage (饲料油菜薹期收获茎秆破碎离散元仿真参数标定), *Transactions of the Chinese Society for Agricultural Machinery*, Madison/Wisconsin, vol.51, no.6, ISSN, pp.73-82.
- [14] Zenghui Gao, Shuqi Shang, Nan Xu, Dongwei Wang., (2022), Parameter calibration of discrete element simulation model of wheat straw-soil mixture in Huang Huai Hai production area, *INMATEH Agricultural Engineering*, Bucharest/Romania, vol.66, no.1, ISSN, pp.201-210.